

Demonstration of Nanofocusing by the use of Plasmonic Lens Illuminated with Radially Polarized Light

Gilad M. Lerman,[†] Avner Yanai, and Uriel Levy*

Department of Applied Physics, The Benin School of Engineering and Computer Science, The Center for Nanoscience and Nanotechnology, The Hebrew University of Jerusalem, Jerusalem, 91904, Israel

Received March 5, 2009; Revised Manuscript Received April 2, 2009

ABSTRACT

We experimentally demonstrate the focusing of surface plasmon polaritons by a plasmonic lens illuminated with radially polarized light. The field distribution is characterized by near-field scanning optical microscope. A sharp focal spot corresponding to a zero-order Bessel function is observed. For comparison, the plasmonic lens is also measured with linearly polarized light illumination, resulting in two separated lobes. Finally, we verify that the focal spot maintains its width along the optical axis of the plasmonic lens. The results demonstrate the advantage of using radially polarized light for nanofocusing applications involving surface plasmon polaritons.

Tight focusing and nanoscale confinement of surface plasmon polaritons (SPPs) is attracting much interest recently. Obtaining subwavelength spot size is desired for enhancing resolution in applications such as microscopy, sensing, and optical memories to name a few. For microscopy and sensing, a smaller spot size allows the achievement of better resolution, such that smaller features and smaller analytes can be observed. For optical memory applications a smaller spot allows one to write smaller bits, thus enabling higher memory density, with the goal of exceeding the current memory density of blu-ray technology (25 GB per layer per disk). A variety of focusing and confinement schemes were proposed and demonstrated over the past few years.^{1–5} For example, SPPs can be focused by the use of plasmonic lens (PL).¹ In its basic form, the PL consists of a single annular subwavelength slit milled into a metal layer. Upon impinging on the slit, the incident wave couples to SPPs propagating through the slit. The SPPs in the slit are then coupled to SPPs that propagate on the upper metal/dielectric boundary and forming a sharp focal spot at the axis of symmetry of the PL. Recently, it was proposed to generate an evanescent Bessel beam by the use of tight focusing of radially polarized light on a dielectric-metal boundary. The tightly focused radially polarized light is TM polarized with respect to this boundary, thus providing cylindrical symmetric focusing.² In another paper, we have theoretically shown that by illuminating a PL with radially polarized light the out of plane electric field

component, which is inherently stronger than the in-plane electric field component, interferes constructively at the optical axis of the PL, thus forming a smaller spot size compared with that achieved by linear polarization illumination.³ We also discussed the role of circular gratings in enhancing the energetic efficiency of the PL.

In this letter, we experimentally demonstrate the focusing of SPPs using a PL illuminated by radially polarized light. We discuss the advantages of using radially polarized light for generating a sharp spot at the optical axis of the PL. We use near-field scanning optical microscope (NSOM) to compare experimentally between SPPs distribution generated by radially and linearly polarized light illumination. We also verify that the spot size is kept nearly constant as we measure the field distribution across planes of different heights above the PL.

Our PL is fabricated by depositing 150 nm thick Ag layer on top of a glass surface followed by a focused ion beam (FIB) milling to define a transparent annular ring in the metal. The ring diameter is 15 μm . The width of the ring is chosen to be 250 nm corresponding to $0.23 \lambda_0$ at our wavelength of operation (Nd:YAG laser, $\lambda_0 = 1064 \text{ nm}$). This slit width was found to be ideal for efficiently generating SPPs at the slit edge,⁶ and for low coupling to radiative modes due to the abrupt termination of the slit.⁷ The linearly polarized beam emerging from the laser is converted to radially polarized beam by the use of space variant nanogratings element. These nanogratings act as a local half-wave plates oriented in such a way to rotate the incident polarization toward the radial direction. More details about the operation

* To whom correspondence should be addressed. E-mail: ulevy@cc.huji.ac.il.

[†] E-mail address: gilad.lerman@mail.huji.ac.il.

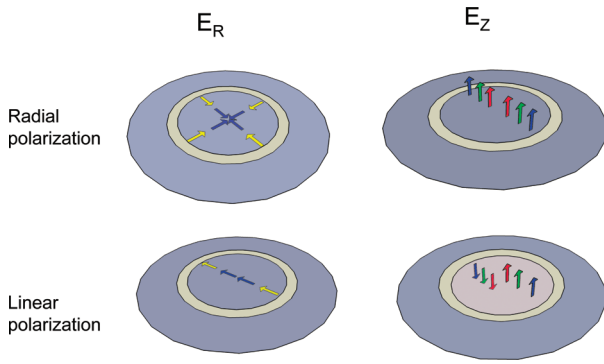


Figure 1. Schematic diagram showing the geometry of the PL and the orientation of the field components under radial and linear polarization illumination.

of this nanogratings element for polarization conversion are given in ref 8.

Radially polarized light beams are the subject of extensive study over the past few years due to their special features such as a tight focal spot and strong longitudinal component of the electric field at the focal plane.^{9–17} The use of radially polarized light for illuminating the PL is preferable over linearly polarized light illumination for the following reasons:

1. As mentioned before, radially polarized light is TM polarized with respect to the annular slit of the PL, whereas the TM component of the linearly polarized light drops as $\cos(\theta)$, where θ is the angle between the polarization direction and the normal to the slit. Keeping in mind that only TM polarization can excite SPPs, it is clear that radially polarized light provides stronger coupling of light into SPPs and strong enhancement of the field at the focus of the PL.
2. The plasmonic lens is essentially a coaxial-like structure. For the specific dimensions and wavelength mentioned above, only the fundamental, radially polarized TEM mode is supported by the structure and can propagate through the 150 nm thick slit. All other modes are beyond cutoff; therefore their transmission efficiency through the subwavelength slit is low.
3. Radially polarized light illumination enables the achievement of a sharper spot at the focus compared with linearly polarized light illumination. This can be intuitively explained by considering the various field components, depicted in Figure 1. For radially polarized light, the in-plane electric field component (E_R) vanishes at the focus due to destructive interference. This can be understood by considering two SPP waves originating from two opposite points along the circumference of the slit and propagating toward the center of the PL. These two SPPs arrive at the focus with the same amplitude and after accumulating the same phase. However, because of the radial field distribution these two SPPs were originated in antiphase and therefore interfere destructively, resulting in a null at the focus. The out-of-plane (longitudinal, with respect to the focusing plane) field component (E_z), however, will interfere constructively at the focus because all SPPs emerging from the slit circumference arrive at the focus with their longitudinal field component pointing

in the same z -direction. This is exactly opposed to the case where the structure is illuminated by a linearly polarized light, where E_R interferes constructively at the focus, and the E_z component interferes destructively. The same is true also for circularly polarized illumination. We now keep in mind that the electrical energy density is proportional to $|E_R|^2 + |E_z|^2$. In contrast to free space focusing, where the ratio between E_z and E_R depends on the numerical aperture of the lens, the SPP mode has a fixed ratio, depending on the dielectric functions of the metal and the dielectric: $|E_z|^2/|E_R|^2 = |k_R|^2/|k_z|^2 = |\epsilon_M/\epsilon_D| > 1$, where $k_{R,z}$ are the SPP k -vectors in the in-plane and the out-of-plane directions, respectively, and ϵ_M , ϵ_D are the permittivities of the metallic and dielectric media respectively. $|\epsilon_M/\epsilon_D| > 1$ because $-\text{Re}(\epsilon_M) > \epsilon_D$ is a necessary condition for the existence of an SPP mode. As a result, the electric energy density is expected to be sharply focused under radial polarization illumination, compared with the case of linear polarization, where the energy density distribution is dominated by a two-lobe pattern along the opposite sides of the PL axis of symmetry, and the case of circular polarization illumination, where the energy density distribution is dominated by a donut shape pattern.

After polarization conversion, the beam is weakly focused onto the sample, which is situated on the stage of an inverted microscope, by a $4\times$ objective lens. The sample is raster scanned by a near-field scanning optical microscope (NSOM, Nanonics Imaging Ltd.) using a probe with 300 nm diameter aperture. The light collected by the probe is guided by the optical fiber onto an InGaAs femtowatt detector (Agilent HP 81634B). Using the feedback mechanism of the NSOM system the probe is kept in contact with the sample (tapping mode) or within a constant distance from it (constant height mode).

Previous studies showed that the in-plane field component couples more efficiently to the aperture NSOM probe compared with the out-of-plane field component.^{1,18} This may jeopardize our goal of measuring the dominant E_z component. The half-cone angle of the probes used in our experiments is $\sim 15^\circ$. For such probes, it is predicted that the power coupling efficiency of the in-plane field is ~ 30 times stronger as compared with that of the out-of-plane field component, that is, $|E_R|^2/|E_z|^2 \sim 30$.¹⁸ Therefore, it is important to choose the experimental parameters such that the ratio of the energy densities resulted from the E_z and E_R components is at least in this range. For an SPP mode, this ratio is determined by the dielectric constants of the metal (ϵ_m) and the dielectric (ϵ_d), as $|E_z|^2/|E_R|^2 = |\epsilon_m/\epsilon_d|$. At our wavelength of operation ($\lambda_0 = 1064$ nm), the dielectric function of Ag is $\epsilon_m = -52 + 3.5i$, thus the ratio $|E_z|^2/|E_R|^2$ is ~ 52 , meaning that despite of the weak coupling of E_z to the probe, the measured intensity is still expected to correspond mostly to $|E_z|^2$. The dominance of the E_z component can be further improved by screening of probes. For imperfect probes with sharp perturbations, the relative coupling efficiency of the E_z component (compared with that of the E_R component) may be increased. We performed

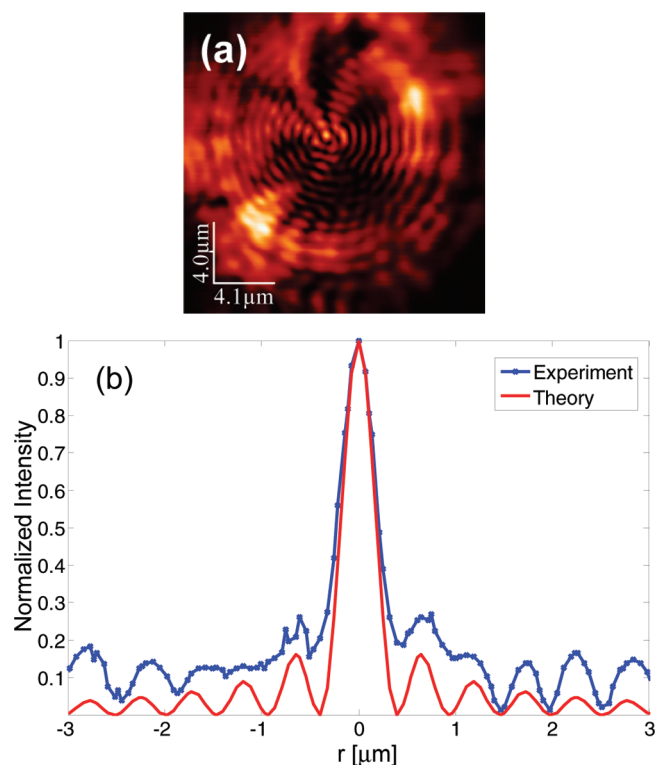


Figure 2. NSOM measurement showing SPP focusing in the plasmonic lens illuminated by radially polarized light. The NSOM probe was at a constant height of $2\ \mu\text{m}$ above the PL. (a) 2D NSOM scan. Bright regions correspond to high intensity. (b) Normalized experimental (blue, cross markers) and theoretical (red, solid line) cross sections through the center of the PL. The sharp focus can be clearly observed.

several scans of the PL under radial polarization illumination with alternating probes and chose those showing dominance of the E_z component (see Supporting Information). A typical two-dimensional (2D) NSOM measurement of the PL illuminated by radially polarized light is presented in Figure 2a. Figure 2b depicts a measured cross section going through the center of the PL. This NSOM scan was performed at a constant height of $2\ \mu\text{m}$ above the sample in order to avoid the damage of the Ag film by the probe. The decay length of the SPP field into the air is $\sim 1.2\ \mu\text{m}$ so that SPPs can be detected at $2\ \mu\text{m}$ height with decent signal-to-noise ratio (see Supporting Information). As expected, it can be seen that SPPs are generated from all directions along the PLs annular slit, forming a set of concentric rings with equal phase, propagating toward the center of the PL and forming a sharp focus. The field distribution of the E_z field is expected to be proportional to the Bessel function $J_0(K_{\text{SPP}}r)$ where $K_{\text{SPP}} \approx 2\pi/1.055\ [1/\mu\text{m}]$ is the propagation constant of the SPP wave and r is the transverse coordinate in cylindrical coordinate system. For comparison purposes, this theoretical cross section is also shown in Figure 2b. The profile of the $(J_0)^2$ function can be clearly observed. Neglecting the contribution of the E_R component, the theoretical spot size (based on full width half-maximum criterion) is $\sim 380\ \text{nm}$. The measured spot size is slightly larger, $410 \pm 39\ \text{nm}$ (error was estimated by taking several cross sections through the center of the PL along different directions). The slight difference may be

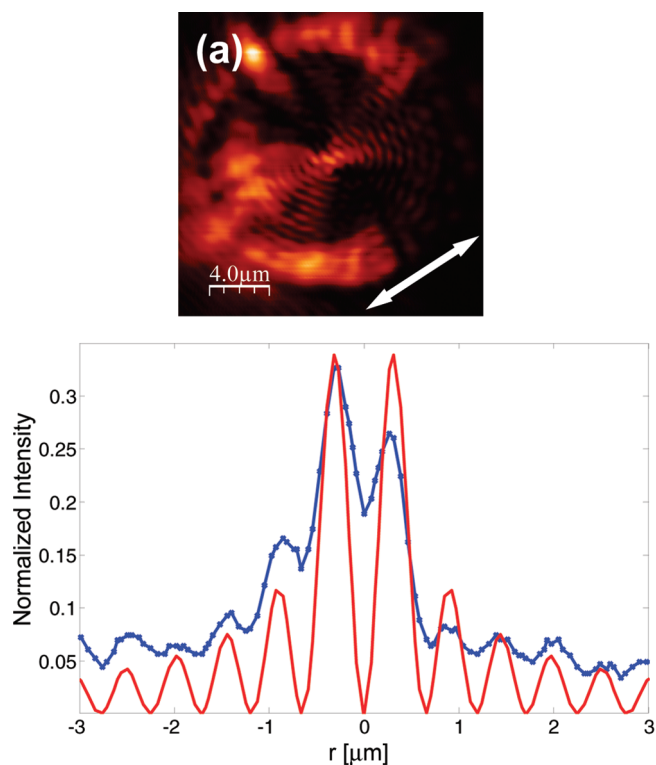


Figure 3. NSOM measurement showing SPP focusing in the plasmonic lens illuminated by linearly polarized light. The NSOM probe was at a constant height of $2\ \mu\text{m}$ from the PL. (a) 2D NSOM scan. Bright regions correspond to high intensity. The white arrow shows the polarization direction of the illuminating field. (b) Normalized experimental (blue, cross markers) and theoretical (red, solid line) cross sections through the center of the PL. Two distinct lobes appear instead of a single focal spot.

attributed to the interaction of the SPP field with the finite aperture size of the probe ($300\ \text{nm}$) and to the existence of E_R component in the measurement.

To demonstrate the importance of polarization in illuminating the PL, we repeat the measurement shown in Figure 2, where the PL is now illuminated by a linearly polarized light. Figure 3a,b shows the 2D NSOM measurement and the cross section going through the center of the PL respectively. One can clearly notice the preferential direction for SPPs generation, which coincides with the polarization direction of the illuminating beam (marked by the arrow in Figure 3a). This is because SPPs are generated only by the polarization component that is perpendicular to the slit.

In contrast to the case of radially polarized illumination, the propagating SPPs do not form a sharp focus at the center of the PL. Instead, a pattern of two separate lobes centered across the PLs axis of symmetry is formed. As explained before, this is due to the destructive interference of the E_z component at the center of the PL. Neglecting contribution of the E_R component, the theoretical field distribution is now proportional to $J_1(K_{\text{SPP}}r)\cos(\theta)$. A cross section of the theoretical intensity profile along the center of the PL is also given in Figure 3b. As can be seen, the experimental and the theoretical curves are in qualitative agreement. Yet, the experimental curve does not show a complete null at the

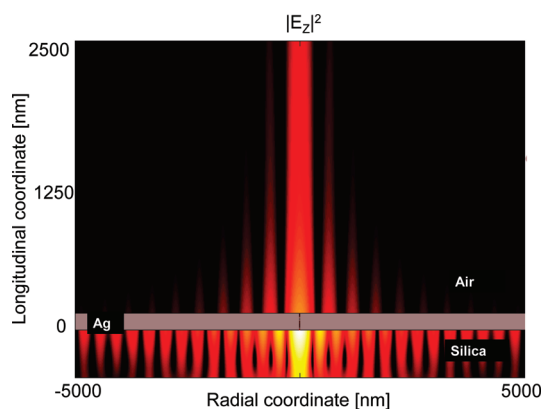


Figure 4. Simulation results showing the longitudinal electrical energy density ($|E_z|^2$) in the r - z plane. Beam lateral profile is nearly constant along the z - (height) axis.

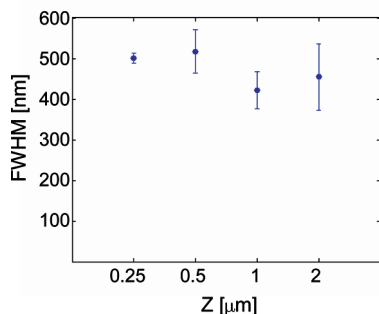


Figure 5. Measured spot size vs height. The error bars were estimated by taking several cross sections through the center of the PL along different directions. The focal spot maintains its width along the optical axis of the PL.

center of the PL. We suspect that this is a result of non-negligible E_r component that is present in the measurement.

As discussed before, the dominant out of plane field distribution of the SPP propagating across the PL, which is illuminated by radially polarized light is proportional to a zero-order Bessel function. Such a field distribution is known to generate the so-called “non-diffracting beam”.¹⁹ Therefore, we expect the spot size to be constant over a range of distances above the PL. To confirm this hypothesis we performed an FDTD simulation of SPP propagation through the PL. Results are shown in Figure 4. As can be seen, a “light bullet” is formed, that is, the spot size is nearly constant along the z -axis. From the simulation, we found the full width at half-maximum (FWHM) of the beam to be 390 nm (slightly above the 380 nm predicted from the distribution of a zero-order Bessel function), with a negligible variation over a range of three microns above the plasmonic lens. In principle, the spot size could be affected by cylindrical waves emerging from the slit.²⁰ However, our simulation shows that the contribution of cylindrical waves is negligible. To validate the simulation results, we performed several NSOM scans at several height levels (250, 500, 1000, and 2000 nm) above the PL. From each NSOM scan, we found the FWHM of the focal spot. Results are shown in Figure 5. Unfortunately, the original probe was broken during the measurements, and the spot sizes obtained with the replacement probe were slightly higher compare with the previous probe, probably

because of higher coupling ratio of E_r/E_z . Yet, in spite of the slight deviation in absolute values, it is still possible to observe non-diffractive beam characteristics, as the measured spot size does not show any significant increase with the increase of height.

In conclusions, we demonstrated tight focusing of SPP waves using a PL that is illuminated by radially polarized light. The field pattern corresponds mostly to the zero-order Bessel function. A spot size of $\sim 0.38 \lambda_0$ was measured. It was shown that the polarization of the illuminating field plays a crucial role in achieving tight focusing. Radial polarization illumination allows to achieve a sharp focus with high energy density, resulting from the constructive interference of the out-of-plane field component at the optical axis and from the symmetric SPP contribution from all azimuthal angles along the annular slit. In contrast, under linear polarization illumination the SPPs are generated mostly from regions where the incident polarization is TM polarized with respect to the slit. Moreover, linear polarization illumination cannot produce a sharp focus. Instead, it generates a two lobe pattern at the two sides of the PL axis of symmetry. Finally, we verified that the focal spot maintains its width along the optical axis of the PL. This long depth of focus is desired for applications such as optical memories where the recording media is at a constant height above the lens²¹ and sensing of analytes that are contained in a solution at some distance above the lens. For such applications, the long depth of focus relaxes the requirement for close proximity between the PL and the medium. The results demonstrate the importance of using radially polarized light illumination for nanofocusing applications involving surface plasmon polaritons.

Acknowledgment. The authors thank Asaf Klein for generating the ring patterns using the FIB tool, Rami Gabay for his assistance in metal deposition, and Yigal Lilach for his assistance in the fabrication of the polarization converter. We acknowledge the financial support of the Israeli Science Foundation, the Israeli Ministry of Science, Culture, and Sport, and the Peter Brojde Center for Innovative Engineering and Computer Science. G.M.L. gratefully acknowledges the support of the Eshkol Fellowship.

Supporting Information Available: This material is available free of charge via the Internet at <http://pubs.acs.org>.

References

- (1) Liu, Z. W.; Steele, J. M.; Srituravanich, W.; Pikus, Y.; Sun, C.; Zhang, X. Focusing surface plasmons with a plasmonic lens. *Nano. Lett.* **2005**, *5*, 1726–1729.
- (2) Zhan, Q. Evanescent Bessel beam generation via surface plasmon resonance excitation by a radially polarized beam. *Opt. Lett.* **2006**, *31*, 1726–1728.
- (3) Yanai, A.; Levy, U. Plasmonic focusing with a coaxial structure illuminated by radially polarized light. *Opt. Express* **2009**, *17*, 924–932.
- (4) Stockman, M. I. Nanofocusing of optical energy in tapered plasmonic waveguides. *Phys. Rev. Lett.* **2004**, *93*, 137404.
- (5) Verhagen, E.; Polman, A.; Kuipers, L. K. Nanofocusing in laterally tapered plasmonic waveguides. *Opt. Express* **2008**, *16*, 45–57.
- (6) Lalanne, P.; Hugonin, J. P.; Rodier, J. C. Theory of surface plasmon generation at nanoslit apertures. *Phys. Rev. Lett.* **2005**, *95*, 263902.
- (7) Ginzburg, P.; Orenstein, M. Plasmonic transmission lines: from micro to nano scale with $\lambda/4$ impedance matching. *Opt. Express* **2007**, *15*, 6762–6767.

- (8) Lerman, G. M.; Levy, U. Generation of a radially polarized light beam using space-variant subwavelength gratings at 1064 nm. *Opt. Lett.* **2008**, *33*, 2782–2784.
- (9) Lerman, G. M.; Levy, U. Effect of radial polarization and apodization on spot size under tight focusing conditions. *Opt. Express* **2008**, *16*, 4567–4581.
- (10) Quabis, S.; Dorn, R.; Eberler, M.; Glöckl, O.; Leuchs, G. Focusing light to a tighter spot. *Opt. Commun.* **2000**, *179*, 1–7.
- (11) Dorn, R.; Quabis, S.; Leuchs, G. Sharper Focus for a Radially Polarized Light Beam. *Phys. Rev. Lett.* **2003**, *91*, 233901.
- (12) Zhan, Q.; Leger, J. R. Focus shaping using cylindrical vector beams. *Opt. Express* **2002**, *10*, 324–331.
- (13) Levy, U.; Tsai, C. H.; Pang, L.; Fainman, Y. Engineering space-variant inhomogeneous media for polarization control. *Opt. Lett.* **2004**, *29*, 1718–1720.
- (14) Kozawa, Y.; Sato, S. Focusing property of a double-ring-shaped radially polarized beam. *Opt. Lett.* **2006**, *31*, 820–822.
- (15) Hao, B.; Leger, J. Experimental measurement of longitudinal component in the vicinity of focused radially polarized beam. *Opt. Express* **2007**, *15*, 3550–3556.
- (16) Youngworth, K. S.; Brown, T. G. Focusing of high numerical aperture cylindrical vector beams. *Opt. Express* **2000**, *7*, 77–87.
- (17) Niv, A.; Biener, G.; Kleiner, V.; Hasman, E. Manipulation of the Pancharatnam phase in vectorial vortices. *Opt. Express* **2006**, *14*, 4208–4220.
- (18) Grosjean, T.; Courjon, D. Polarization filtering induced by imaging systems: Effect on image structure. *Phys. Rev. E* **2003**, *67*, 046611.
- (19) Durnin, J. Exact solutions for nondiffracting beams. I. The scalar theory. *J. Opt. Soc. Am. A* **1987**, *4*, 651–654.
- (20) Aigouy, L.; Lalanne, P.; Hugonin, J. P.; Julié, G.; Mathet, V.; Mortier, M. Near-Field Analysis of Surface Waves Launched at Nanoslit Apertures. *Phys. Rev. Lett.* **2007**, *98*, 153902.
- (21) Srituravanich, W.; Pan, L.; Wang, Y.; Sun, C.; Bogoy, D. B.; Zhang, X. Flying plasmonic lens in the near field for high-speed nanolithography. *Nat. Nanotechnol.* **2008**, *3*, 733–737.

NL900694R